A Study on REMPI as a Measurement Technique for Highly Rarefied Gas Flows* (Simulations and Its Fundamental Properties of REMPI Spectra)

Hideo MORI**, Toshihiko ISHIDA**,
Shigeyuki HAYASHI**, Yoshinori AOKI**
and Tomohide NIIMI**

Nowadays, a non-intrusive measurement tool of thermodynamic variables with high sensitivity is strongly demanded for analyses of highly rarefied gas flows. REMPI (resonantly enhanced multiphoton ionization) is the most suitable technique for measurement of gas molecules with very low density. In this study, to examine the fundamental properties of the REMPI spectra, 2R+2 N_2-REMPI spectra including the spectral broadening are calculated and compared with the experimental results. From the calculated REMPI spectra, spectral lines adequate to measure temperature are proposed, especially at relatively high temperature where the measurement error becomes larger because of the overlap of the spectral lines.

Key Words: Rarefied Gas, Flow Measurements, Laser-aided Diagnostics, REMPI, Nitrogen, Spectral Simulation

1. Introduction

Nowadays, analyses of highly rarefied gas flows are strongly demanded for depelopment of vacuum science and aerospace engineering. For example, to diagnose material surfaces for ultra-high vacuum devices, such as electropolishing and oxidation, we have to examine not only static properties of amount of gas molecules desorbed from solid surfaces, but also behaviors of gas molecules interacting with these surfaces such as energy transport processes. In the space engineering, impingement of exhaust gas jets from satellite thrusters on the solar battery panels or antennae is also a serious problem including interaction of very cooled gas molecules with these surfaces and contamination of the exhaust gas molecules.

So far, mass spectrometers and Patterson probes have been used to measure number density of rarefied gas flows, but these method cannot measure nonequilibrium among internal (translational, vibrational, and rotational) energy. This means that the molecular energy transport processes between gas molecules and solid surfaces cannot be examined precisely.

On the other hand, the necessity of non-intrusive measurement of thermodynamic variables has motivated the development of spectroscopic techniques, such as electron beam fluorescence (EBF)[1], laser induced fluorescence (LIF)[2], and coherent anti-Stokes Raman scattering (CARS)[3]. These spectroscopic methods have enabled to detect the nonequilibrium in rarefied gas flows, because they are based on internal energy distributions of gas molecules obtained from the spectral profiles. Figure 1 shows the applicable range of number density for several optical techniques. Since these techniques are based on the detection of fluorescence or scattering light, even LIF, which is the most sensitive method among them, is difficult to be applied to the rarefied gas flow below 10^{12} molecules/cm^3.

For non-intrusive measurement with high sensitivity, a REMPI (Resonantly Enhanced Multiphoton

* Received 7th March, 2000. Japanese original: Trans. Jpn. Soc. Mech. Eng., Vol. 65, No. 637, B (1999), p. 3035-3041 (Received 21st December, 1998)

** Department of Electronic-Mechanical Engineering, Nagoya University, Furo-cho, Chikusa, Nagoya, Aichi 464-8603, Japan. E-mail: mori@suelab.nuem.nagoya-u.ac.jp

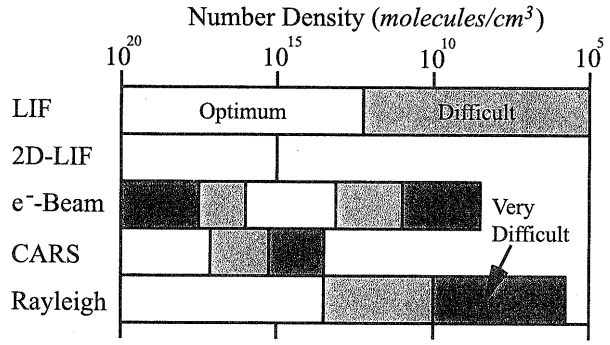

Fig. 1 Optical diagnostics application regimes

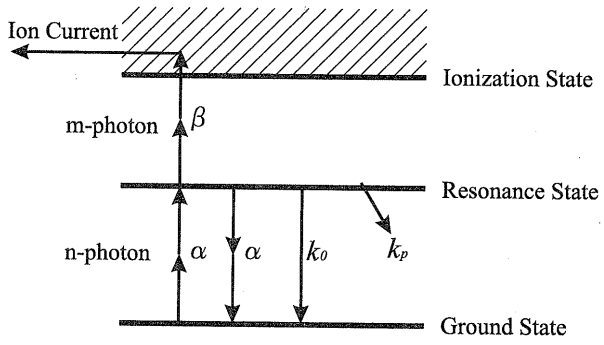

Fig. 2 Modeling of $nR+m$ REMPI process

Ionization) technique is the most suitable, allowing measurement of thermodynamic variables of highly rarefied gas flows. In the REMPI technique, ions excited to the ionization state from the ground state by multiple photons are detected as a signal and its spectra depending on the wavelength of laser beam are analysed to measure temperature. In general, photoionization of gas molecules using multiple photons has very low transition probability. Using REMPI method, however, high transition probability can be established because gas molecules pass through the resonance state before ionization. Although REMPI has been established as a detection technique with high sensitivity for molecules such as N_2 and H_2 which cannot be directly excited to the resonance state by one photon, an attention has been paid to REMPI recently as a very sensitive measurement technique for highly rarefied gas flows. In the case of N_2, the detection limit of 10^9 molecules/cm^3 for 2R+2 REMPI[4], and 10^5 molecules/cm^3 for 2R+1 REMPI[5] have been reported (see the next chapter for meanings of 2R+2 and 2R+1).

To apply REMPI to measurement of thermodynamic variables in highly rarefied gas flows, fundamental properties of REMPI spectra have to be examined, such as its dependence on temperature and density of gas molecules. Moreover, it is also important to determine which spectral lines are appropriate for Boltzmann plot to measure rotational temperature accurately. In this study, we develop the simulation code of 2R+2 REMPI spectra considering Doppler and collision broadening and laser linewidth, and examine the fundamental properties of REMPI spectra by the simulations. As a carrier gas we employ N_2 which is the main constituent of air and one of the main constituent of exhaust gas of satellite thrusters. Firstly, a basic process of REMPI is described using rate equations and the dependence of 2R + 2 N_2-REMPI signal intensity on laser flux is clarified. Secondly, the calculation method for 2R + 2 N_2-REMPI spectra is presented considering the rotational strength (two-photon Hönl-London factor), the spectral broadening (Voigt profile and laser linewidth) and so on, and the calculated spectra are compared with the experimental ones measured on the center line of the free molecular flow issued from a sonic nozzle. Finally, we propose the spectral lines adequate to measure temperature accurately by Boltzmann plot, especially at relatively high rotational temperature where the measurement error becomes larger because of the overlap of the spectral lines. The selection of the vibration band is also suggested to detect the signal with high S/N.

2. Theory of REMPI

2.1 Modeling of REMPI process

Figure 2 shows a model of a nR+m REMPI process in which molecules in the ground state are excited to the resonance state by n photons, and then they are ionized by m photons.

Rate equations for the REMPI process are given by[6]

$$dX/dt=-\alpha X+(\alpha+k_0)R, \quad (1)$$

$$dR/dt=\alpha X-(\alpha+k_0+k_p+\beta)R, \quad (2)$$

$$dC/dt=\beta R, \quad (3)$$

where X, R, and C are number density of molecules at the ground, resonance, and ionization state, respectively. α is the n-photon stimulated absorption constant, and β is the m-photon ionization constant. They can be defined as $\alpha\equiv\delta_n^{(r)}F^n$ and $\beta\equiv\delta_m^{(i)}F^m$, respectively, if using laser flux F, the n-photon absorption cross section $\delta_n^{(r)}$, and the m-photon ionization cross section $\delta_m^{(i)}$. k_0 is the one-photon, spontaneous emission constant of the resonance state, and k_p is the spontaneous, irreversible decay constant of the resonance state.

Assuming the population of resonant level is constant[7], from Eq.(2) R is given by

$$R=\frac{\alpha}{\alpha+\beta+k_0+k_p}X. \quad (4)$$

Substituting R into Eq.(3) and assuming the condition $\alpha\ll\beta$, ion current I is given by

$$I\propto\frac{dC}{dt}=\frac{\alpha\beta}{\beta+k_0+k_p}X$$

$$= \frac{X\delta_n^{(r)}\delta_m^{(i)}F^{n+m}}{\delta_m^{(i)}F^m + k_0 + k_p.} \quad (5)$$

At the limit of the low laser flux ($\delta_m^{(i)}F^m \ll k_0, k_p$), I is given approximately by

$$I \propto \frac{X\delta_n^{(r)}\delta_m^{(i)}}{k_0 + k_p}F^{n+m}. \quad (6)$$

When the population of the ground state X is constant, I depends on F^{n+m}. On the other hand, when the laser flux is moderately high under the condition of negligible depletion of the ground state and it is assumed that $\delta_m^{(i)}F^m \gg k_0$ and k_p, I leads to the following,

$$I \propto X\delta_n^{(r)}F^n, \quad (7)$$

showing the dependence of I on F^n. In this case, since the REMPI spectra reflects only the n-photon transition from the ground state to the resonance state[7], this leads to easier analysis of the REMPI spectra for the measurement of rotational temperature.

2.2 N_2-REMPI

In this study, nitrogen is used as carrier gas to examine the fundamental properties of REMPI, because it is the main constituent of air and one of the main constituent of exhaust gas components for satellite thrusters. For N_2-REMPI, three types of schemes, 2R+2, 2R+1 and 3R+1, have been reported, and the former two schemes have been widely employed. Ground-level molecules are excited to the $a^1\Pi_g$ (the Lyman-Birge-Hopfield system) and the $a''^1\Sigma_g^+$ state for 2R+2 and 2R+1 REMPI, respectively. In the latter case, in addition to high sensitivity, only the Q branch is enhanced because of a $^1\Sigma_g^+ - {}^1\Sigma_g^+$ transition for linearly polarized light, leading to easy assignment of the spectra. Moreover, as the rotational transition strength is independent of J, it is easy to measure rotational temperature from the spectra. However, since 2R+1 N_2-REMPI needs a laser source whose wavelength is around 200 nm, a complicated optical system including a frequency tripled dye laser has to be provided. Further, there is a problem that the intensity of laser beam will decrease, because O_2 molecules in air have absorption lines around 200 nm. In this study, therefore, we employ 2R+2 N_2-REMPI because of its easy optical arrangement and no consideration of O_2-absorption.

3. Simulation of REMPI Spectra

3.1 Spectral line intensities of REMPI

When the laser power is constant, the rotational line intensity in REMPI spectra is given by[4),(8)]

$$I_{J',J''} = Cg(J'')S(J',J'')\exp(-E_{rot}/kT_{rot}). \quad (8)$$

In this equation, C is a constant independent of the rotational quantum number J, including Franck-Condon factor, laser flux, number density of the molecules, and so on. $g(J'')$ is the nuclear statistical factor.

Table 1 Two-photon Hönl-London factors of N_2 for the $a^1\Pi_g \leftarrow X^1\Sigma_g^+$ transition using linearly polarized light

	Branch	$S(J',J'')$
O	$(\Delta J=-2)$	$M(O)J''(J''-2)/15(2J''-1)$
P	$(\Delta J=-1)$	$M(P)(J''+1)/30$
Q	$(\Delta J=0)$	$M(Q)(2J''+1)/10(2J''-1)(2J''+3)$
R	$(\Delta J=1)$	$M(R)J''/30$
S	$(\Delta J=2)$	$M(S)(J''+1)(J''+3)/15(2J''+3)$

For N_2^{14}, $g(J'')$ is 3 and 6 for odd and even J'', respectively. $S(J',J'')$ is the rotational transition strength (two-photon Hönl-London factor), which depends on the electronic angular momentum Ω about the internuclear axis and on the polarization (linear or circular) of laser beam. In Table 1, two-photon Hönl-London factors for the $a^1\Pi_g \leftarrow X^1\Sigma_g^+$ transition by linearly polarized light[9)-(11)] are listed. The $M(O)$-$M(S)$ in Table 1 are the transition dipole factors given by products of the electronic dipole transition moments, and they depend on the kind of the branches. However, since they are independent of J, they can be considered as constants[10)] when the spectral lines of REMPI in the same branch are analysed.

The exponential term in Eq.(8) is the Boltzmann factor originating from the rotational population; k is the Boltzmann's constant, T_{rot} the rotational temperature, and E_{rot} the rotational energy. Plotting $\ln(I/gS)$ versus E_{rot}/k according to the above equation, rotational temperatures can be easily derived from its slope $-T_{rot}^{-1}$ (Boltzmann plot). Instead of the Boltzmann plot, rotational temperature can be also measured by best fitting of the simulated spectra to experimental ones.

3.2 Intensitiy of vibrational bands

In this study, we use (1, 0) band to examine the fundamental properties of the N_2-REMPI signals and to compare with the experimental ones[12)]. The (1, 0) band basically shows the same properties as another band, e.g., (2, 0) or (3, 0) band. For detection of the N_2-REMPI signal with a high ratio of signal to noise, however, it is desirable to select the most intense vibrational band, leading to accurate measurement of the rotational temperature. The relative strength of the REMPI signal among vibrational bands depends on the Franck-Condon factor, which is included in C of Eq.(8). For (1, 0), (2, 0), (3, 0), and (4, 0) bands, the Franck-Condon factors for the $a \leftarrow X$ transition are 0.1155, 0.1707, 0.1832, and 0.1600, respectively[13)]. Therefore, it is better to use (2, 0) or (3, 0) band for N_2-REMPI experiments.

3.3 Effects of line broadening

Actually, no spectral lines in experimental REMPI spectra are monochromatic. The spectral

lines are broadened by collision and Doppler broadening and the laser linewidth. Therefore, to examine the effects of these broadening and the spectral overlaps on the Boltzmann plot, we have to calculate the REMPI spectra considering these effects. Also, for temperature measurement using the best fitting instead of the Boltzmann plot, these broadening should be considered. The Voigt profile[14] is employed for the each line to calculate the effects of both collision and Doppler broadening. Then the convolution of these line broadening and the laser profile is calculated to simulate the realistic REMPI spectra.

Voigt profile is given by:

$$g(\nu)=\frac{y}{\pi\Delta\nu_D}\sqrt{\ln 2\pi}\int_{-\infty}^{+\infty}\frac{\exp(-t^2)}{y^2+(x-t)^2}dt, \qquad (9)$$

where x and y are defined by

$$y=\frac{\Delta\nu_c}{\Delta\nu_D}\sqrt{\ln 2}, \qquad (10)$$

$$x=\frac{\nu-\nu_0}{\Delta\nu_D}\sqrt{\ln 2}. \qquad (11)$$

ν_0 is the resonance frequency of the absorption line.

$\Delta\nu_c$ and $\Delta\nu_D$ in Eqs.(9)-(11) are collision and Doppler width (full width at half maximum: FWHM), respectively[14],[15].

4. Results and Discussions

4.1 Comparison of calculated spectra to experimental ones

4.1.1 Conditions of experiment and simulation

We compared the calculated REMPI spectra with the experimental ones[12] to check whether the simulation method mentioned in the previous chapter is appropriate. The experimental spectra is measured at the centerline of the free molecular flow issued from a sonic nozzle. To simulate the REMPI spectra in the free molecular flow, it is necessary for calculation of Voigt profile to obtain translational temperature and pressure in advance. Both values are determined from isentropic flow relations through Mach number along the centerline of the jet[16], which is calculated from the empirical equation given by Ashkenas and Sherman[17]. The stagnation pressure and the temperature are kept at 3750 Torr and 300 K, respectively.

The input laser intensity profile is assumed to be gaussian, and the laser linewidth is decided to be 1.4 cm^{-1} by fitting the calculated spectra to the experimental one (Fig. 3) at S(1) and S(2), considering the collision and Doppler broadening.

The experimental REMPI spectra and the calculated ones shown in Figs. 3 and 4 are obtained at $x/D=17$ and 83, respectively. The spectra at the bottom of these figures are calculated at 16.2 K and 7.5 K which are deduced from the Boltzmann plot (Fig. 5) of the peak values at S(1), S(2), S(3) and S(4) of the experimental spectra.

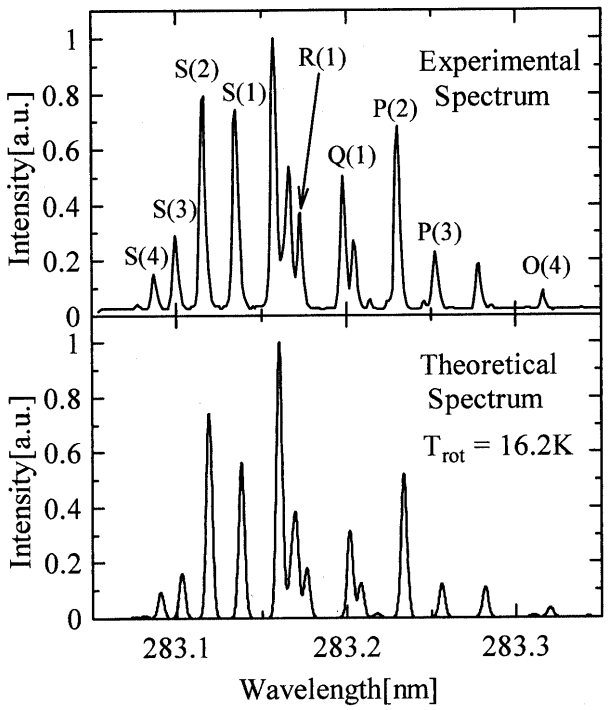

Fig. 3 Experimental spectrum at $x/D=17$ compared with the theoretical one at $T_{rot}=16.2$ K

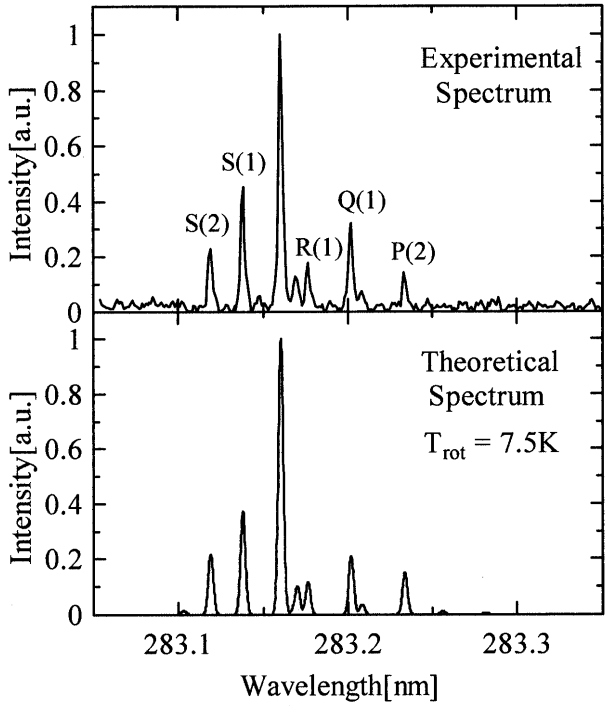

Fig. 4 Experimental spectrum at $x/D=83$ compared with the theoretical one at $T_{rot}=7.5$ K

4.1.2 Effect of collision and Doppler broadening

At $x/D=17$ as shown in Fig. 3, the Mach number M_a, the translational temperature T_{tr}, and the pressure p at the focal point result in 11.2, 11.4 K, and 4.05×10^{-2} Torr, respectively. Under these condition, the

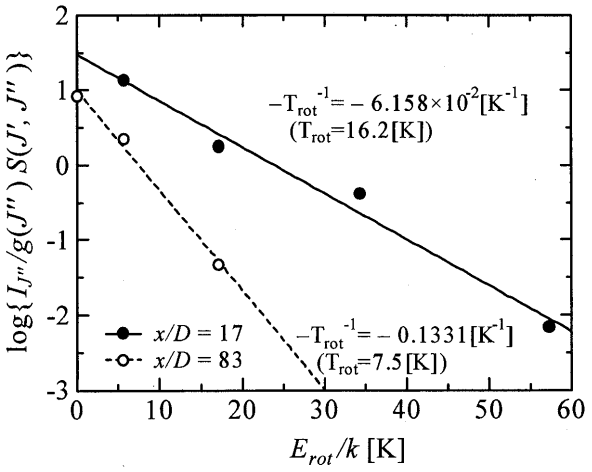

Fig. 5 Boltzmann plot

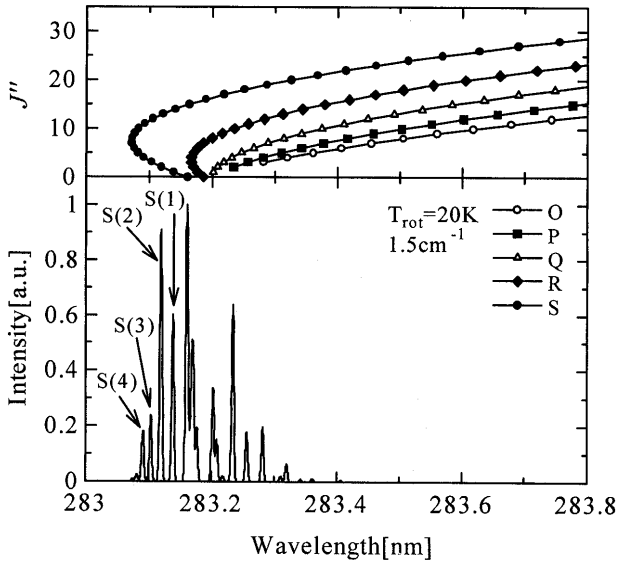

Fig. 6 Simulated REMPI spectrum at T_{rot}=20 K (laser linewidth : 1.5 cm^{-1})

collision and Doppler width are $\Delta\nu_c=1.50\times10^{-5}$ cm^{-1} and $\Delta\nu_D=3.22\times10^{-2}$ cm^{-1}. On the other hand, at $x/D=83$ (Fig. 4), $M_a=21.3$, $T_{tr}=3.26$ K, and $p=5.01\times10^{-4}$ Torr, $\Delta\nu_c=3.47\times10^{-7}$ cm^{-1} and $\Delta\nu_D=1.72\times10^{-2}$ cm^{-1}. Therefore, in the REMPI spectra at low pressure, it is found that the effect of collision broadening is negligible. Further, at very low temperature, since the effect of Doppler broadening also becomes small, the broadening of these REMPI spectra is caused mainly by the laser linewidth (1.4 cm^{-1}).

4.1.3 Comparison between calculated spectra and experimental ones Figures 3 and 4 show that the calculated spectra agree well with the experimental ones, except the relative strength of S(1) and S(2) in Fig. 3. This is because the relative strength of S(1) and S(2) changes critically at very low rotational temperature. Therefore, small error in the deduced temperature causes incorrect relative strength of S(1) and S(2) in the calculated spectra from the experimental one. As shown in Fig. 5, at $x/D=17$, the plotted data deviate from the line fitted by the least square method, so the rotational temperature deduced by the Boltzmann plot may have an error.

It can be seen in Fig. 3 or 4 that relative intensity of two spectral lines each belonging to different branches is incorrect, for example, Q(1) and P(2). This may be caused by no consideration of difference between M's for two branches. Normally, there is no problem because spectral lines belonging to the same branch are used for Boltzmann plot. It should be noted that, when using the fitting method to measure temperature, M values have to be deduced experimentally in advance, comparing the experimental spectra with theoretical ones calculated at known temperature.

4.2 Properties of N_2-REMPI spectra and selection of spectral lines

In this study, the fundamental properties of REMPI spectra such as the dependence on the temperature and the pressure are clarified by the simulated spectra. Moreover, spectral lines adequate to measure the rotational temperature are selected. We assumed that the translational and rotational temperature are equal for the spectra in this section. As shown in previous section, the effect of collision broadening is very small for rarefied gas flows, so the collision broadening is ignored for the spectra shown in this section.

Figures 6, 7, and 8 are simulated 2R+2 N_2-REMPI spectra for (1, 0) band. The laser linewidth is 1.5 cm^{-1}, and the rotational temperature T_{rot} is 20 K, 120 K, and 300 K, respectively. The lower part of each figure shows the REMPI spectrum. The horizontal axis shows the wavelength of the laser and the vertical axis shows the relative intensity normalized by the maximum. The upper part is a Fortrat diagram showing the wavelength of each absorption line. In this diagram, the vertical axis shows the rotational quantum number J'' of the ground state.

As shown in Fig. 6 at $T_{rot}=20$ K, only the spectral lines corresponding to low rotational levels ($J''<5$) appear at extremely low temperature, and these abosorption lines have no overlap with another line. Therefore, lines S(1), S(2), S(3) and S(4) are suitable for the measurement of temperature by the Boltzmann plot.

For $T_{rot}>100$ K, however, since spectral lines become crowded, it is difficult to measure the spectral intensity because of overlap with other lines. In this case, therefore, Boltzmann plot using these lines becomes incorrect. As seen in Fig. 7 for $T_{rot}=120$ K, spectral lines of higher rotational level appear, and

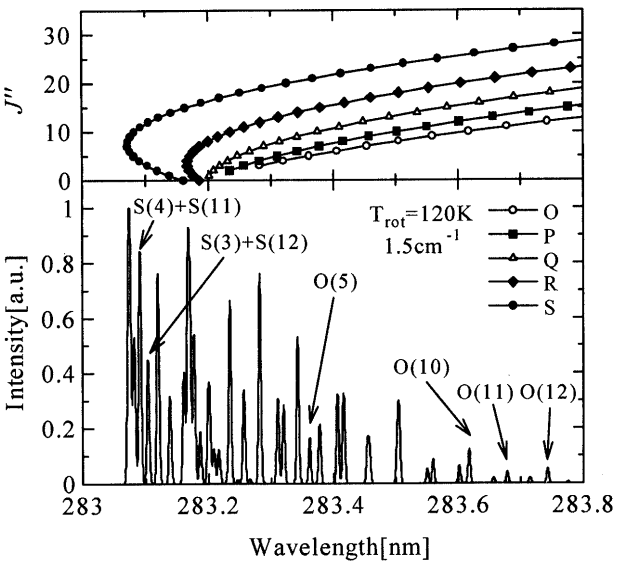

Fig. 7 Simulated REMPI spectrum at T_{rot}=120 K (laser linewidth: 1.5 cm^{-1})

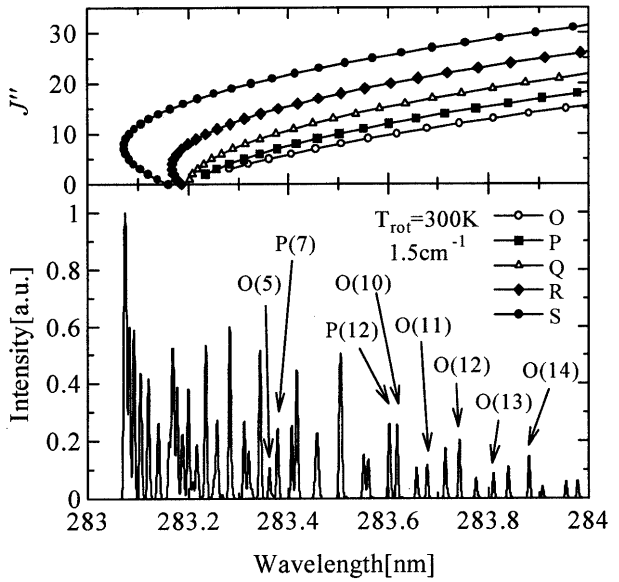

Fig. 8 Simulated REMPI spectrum at T_{rot}=300 K (laser linewidth: 1.5 cm^{-1})

the lines near the band head have overlap with another line. If using the S(1), S(2), S(3) and S(4) to measure rotational temperature, we obtain 134.9 K in spite of the use of the calculated spectra. This error is mainly attributed to that S(12) and S(11) lines coincide with S(3) and S(4), respectively, as shown in the Fortrat diagram (see Fig. 7). Therefore, S branch cannot be used to measure temperature above 100 K. Instead of S branch, O branch including O(5), O(10), O(11) and O(12) is suitable for the measurement of rotational temperature, because these lines separate from any other lines. We deduce rotational temperature from the Boltzmann plot using these lines in this calculated spectra (Fig. 7) and can evaluate the temperature of 120.0 K. In the experimental condition of low S/N, however, there may be a large error in the measured temperature, because the effect of the noise becomes larger at O(11) and O(12) lines whose intensities are relatively low. In this case, the fitting method may be appropriate for the measurement of the rotational temperature.

In the range of a rotational temperature near 300 K, Boltzmann plot using spectral lines of O(5), O(10), O(11) and O(12) also can be used. In this case (See Fig. 8 at T_{rot}=300 K), since intensity of O(13) and O(14) becomes large and these lines are also separated from any other lines, by using these lines additionally for the Boltzmann plot, it is possible to measure rotational temperature more accurately.

We think that integrated intensity values of the spectral lines should be used for the Boltzmann plot. When the effect of overlap of the spectral lines is large, however, the overlap causes errors for the integrated intensity of the lines. As mentioned above, rotational temperature deduced by Boltzmann plot using the simulated REMPI spectra indicates more accurate one when using spectral peak intensity instead of integrated one. In this study, therefore, peak intensity of the spectral lines is used for the Boltzmann plot.

5. Conclusions

In this study, the theory of REMPI and the typical features of N_2-REMPI spectra for highly rarefied gas flows were described, and the calculation method for the REMPI spectra was presented, considering two-photon Hönl-London factor, Franck-Condon factor and the spectral broadening. Following concluding remarks are obtained.

1. To examine the fundamental properties of the REMPI spectra, 2R+2 N_2-REMPI spectra were calculated and compared with the experimental ones successfully.

2. When rotational temperature is measured by the use of 2R+2 N_2-REMPI spectra through the Boltzmann plot, S branch is better for low temperature (near 20 K).

3. For relatively high temperature (>120 K), using S branch for the Boltzmann plot induce some error of temperature because the lines belonging to S branch overlap each other. In this case, O branch is more suitable for the measurement of rotational temperature.

In this study, the vibrational band of (1, 0) is used to elucidate the fundamental properties of the REMPI. For the high S/N measurement, however, (2, 0) or (3, 0) band may be better because they have larger Franck-Condon factors than (1, 0) band.

Acknowledgements

The present work was supported by a grant-in-aid for Scientific Research (B) from the Ministry of Education, Science, Sports and Culture.

References

(1) Dankert, C., Cattolica, R. and Sellers, W., Local Measurement of Temperatures and Concentrations: A Review for Hypersonic Flows, A. Boutier ed., New Trends in Instrumentation for Hypersonic Research, (1994), p. 563-581.

(2) Niimi, T., Fujimoto, T. and Shimizu, N., Method for Planar Measurement of Temperature in Compressible Flow Using Two-line Laser-Induced Iodine Fluorescence, Opt. Lett., Vol. 15-16 (1990), p. 918-920.

(3) Hara, Y., Fujimoto, T., Niimi, T., Fukuda, Y. and Oba, H., Measurement of Temperature and Number Density by CARS: Application to Plasma Jets, Rarefied Gas Dynamics: Space Science and Engineering, AIAA, Vol. 160 (1992), p. 360-370.

(4) Carleton, K.L., Welge, K.H. and Leone, S.R., Detection of Nitrogen Rotational Distributions by Resonant 2+2 Multiphoton Ionization through the $a^1\Pi_g$ State, Chem. Phys. Lett., Vol. 115, No. 6 (1985), p. 492-495.

(5) Lykke, K.R. and Kay, B.D., Two-photon Spectroscopy of N_2: Multiphoton Ionization, Laser-induced Fluorescence, and Direct Absorption via the $a''^1\Sigma_g^+$ State, J. Chem. Phys., Vol. 95, No. 4 (1991), p. 2252-2258.

(6) Zakheim, D.S. and Johnson, P.M., Rate Equation Modelling of Molecular Multiphoton Ionization Dynamics, Chem. Phys., Vol. 46 (1980), p. 263-272.

(7) Goodman, L. and Philis, J., Andrews, D.L., ed., Applied Laser Spectroscopy: Techniques, Instrumentation, and Applications, (1992), p. 319-364, VCH pub.

(8) Niimi, T., Dankert, C. and Nazari, B.K., Resonantly Enhanced Multiphoton Ionization for Analyses of Rarefied Gas Flows - 2R+2 N_2-REMPI -, DLR -IB 223-96 A 42 (1996).

(9) Bray, R.G. and Hochstrasser, R.M., Two-Photon Absorption by Rotating Diatomic Molecules, Mol. Phys., Vol. 31, No. 4 (1976), p. 1199-1211.

(10) Halpern, J.B., Zacharias, H. and Wallenstein, R., Rotational Line Strengths in Two- and Three-Photon Transitions in Diatomic Molecules, J. Mol. Spectrosc., Vol. 79 (1980), p. 1-30.

(11) Bruno, A.E., Schubert, U., Neusser, H.J. and Schlag, E.W., Resonantly Enhanced 2+2 Multiphoton Ionization Spectra of N_2 via the $\tilde{a}^1\Pi_g$ State: A Line Intensity Study, Chem. Phys. Lett., Vol. 131, No. 1-2 (1986), p. 31-36.

(12) Nazari, B.K., Untersuchung von Abgasstrahlen aus Kleintriebwerken mit der Lasermeßtechnik REMPI, DLR-Forschungsbericht 1999-27 (1999).

(13) Trickl, T., Proch, D. and Kompa, K.L., Resonance-Enhanced 2+2 Photon Ionization of Nitrogen: The Lyman-Birge-Hopfield Band System, J. Mol. Spectrosc., Vol. 162 (1993), p. 184-229.

(14) Eckbreth, A.C., Laser Diagnostics for Combustion Temperature and Species, Abacus, (1988).

(15) Smith, A.P., Hall, G., Whitaker, B.J., Astill, A.G., Neyer, D.W. and Delve, P.A., Effects of Inert Gases on the Degenerate Four-wave-mixing Spectrum of NO_2, App. Phys. B, Vol. 60 (1995), p. 11-18.

(16) Matsuo, K., Dynamics of Compressive Fluids, (in Japanese), (1994) Rikogakusha.

(17) Ashkenas, H. and Sherman, F.S., The Structure and Utilization of Supersonic Free Jets in Low Density Wind Tunnels, Proceedings of 4th International Symposium on Rarefied Gas Dynamics, 2, (1966), p. 84-105, Academic Press.